Supporting Information

Biological Phytic Acid as a Multifunctional Curing Agent for Elastomers: Towards Skin-Touchable and Flame Retardant Electronic Sensors

Quanquan Guo, Jie Cao, Yangyang Han, Yumeng Tang, Xinxing Zhang*, and Canhui Lu*

State Key Laboratory of Polymer Materials Engineering, Polymer Research Institute of Sichuan University, Chengdu 610065, China.

E-mail: xxzwwh@scu.edu.cn, canhuilu@scu.edu.cn

Preparation of CNC
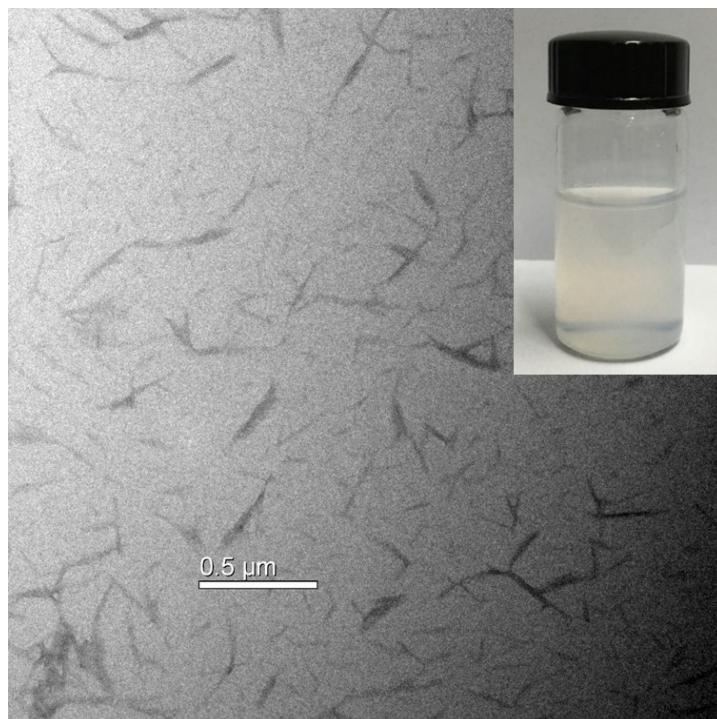
Figure S1. TEM image of CNC suspension. Inset picture gives the digital picture of CNC suspension.

Firstly, cellulose nanocrystal (CNC) suspension was prepared by hydrolyzing cotton with sulfuric acid. Medical purified cotton (20 g) was mixed with sulfuric acid solution (64 wt%, 400 mL) and heated at 45 °C for 45 min. The reaction was immediately quenched by the dilution with deionized water to avoid further hydrolysis. The obtained product was washed with deionized water for 2 times by centrifugation at 50000 rpm for 5 min, and then dialysis was applied to remove residual acid until the dialysate appeared neutral.

Measurement of swelling ratio and cross-link density

The cross-link density was measured by the equilibrium swelling technique in toluene solvent and subsequently calculated according to the classical Flory-Rechner equation.[1] Briefly, the samples tailored with nearly same size were weighed and swelled in toluene at room temperature for 72 h. The swollen samples were removed from the solvent and weighed immediately. Then, the volumes and densities of all swollen samples were measured by the method of pycnometer testing.

The elastically active network chain density, v_e, which was used to represent the cross-link density, was then calculated by the well-known Flory-Rechner equation.[2]

$$v_e = \frac{\rho_d}{M_c} = - \frac{\ln\left(1 - v_r\right) + v_r + \chi v_r^2}{v_s(v_r^{1/3} - v_r/2)}$$

Where v_r is the volume fraction of the polymer in the elastomer swollen to equilibrium, v_s is the solvent molar volume (106.3 cm^3/mol for toluene), and χ is the rubber-toluene interaction parameter and is taken as 0.0653.

Swelling ratios of ENR elastomers were calculated using equation below

$$S = \frac{m_1 - m_0}{m_0}$$

Where m_0 and m_1 are initial weight and the weight of the swollen samples, respectively.

Table S1. The experimental vulcanization formula for preparation of S-cured ENR

Component	Sulphur	Zinc oxide	Stearic acid	CBS	OP emulsifier-10
Content (phr)	1.68	3.00	1.80	0.90	0.25

Table S2. Mechanical properties of PA-cured ENR and S-cured ENR

Sample	ENR-0%	ENR-10%	ENR-20%	ENR-30%	ENR-40%	ENR-S
Tensile strength (MPa)	2.51	5.72	7.63	9.66	11.15	11.62
Young's modulus (MPa)	0.55	0.93	1.29	1.71	2.04	3.69
Elongation at break (%)	1223.89	1466.67	1428.06	1375.00	1328.89	960.83

Table S3. UL-94 testing results of PA-cured ENR

Content of PA (phr)	Vertical flame test		Melt dripping	Rating
	After the first 10 s ignition	After the second 10 s ignition		
0	No extinction	-	Yes	No rating
10	Extinction	Fast combustion	Yes	No rating
20	Extinction	Burning	Yes	V-2
30	Extinction	Slow combustion	Yes (the slowest speed)	V-1
40	Extinction after ignition	Extinction after 6 s	No	V-0

DMA
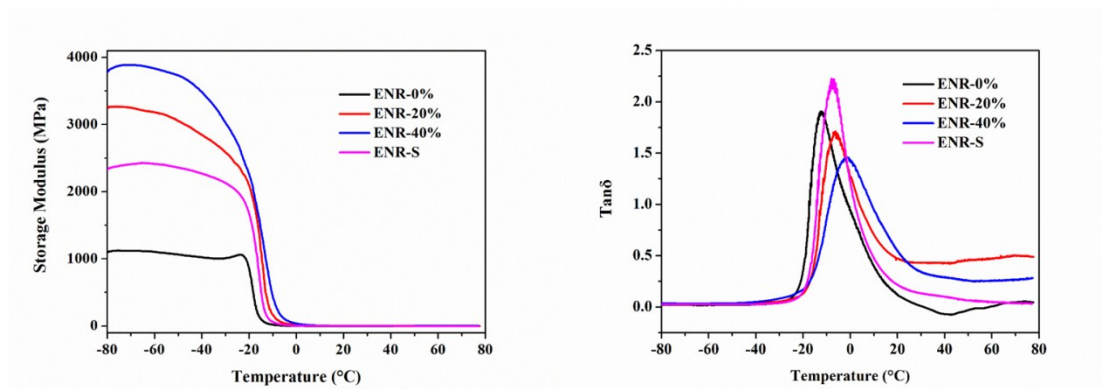
Figure S2. Storage modulus (left) and tanδ (right) of ENR cured by PA and S.

DMA was also conducted to verify the cross-linking of ENR by PA. The DMA curves of ENR cured by PA and S are shown in **Figure S2**. The storage modulus of ENR increases significantly with increasing PA content due to the formation of covalent cross-link network. Moreover, the storage modulus of 40 wt% PA-cured ENR is higher than that of S-cured ENR. The glass-transition temperature of ENR shifts to a higher temperature with increasing PA content. The above-mentioned results all suggest the successful construction of a covalent bonds cross-link network in ENR matrix.
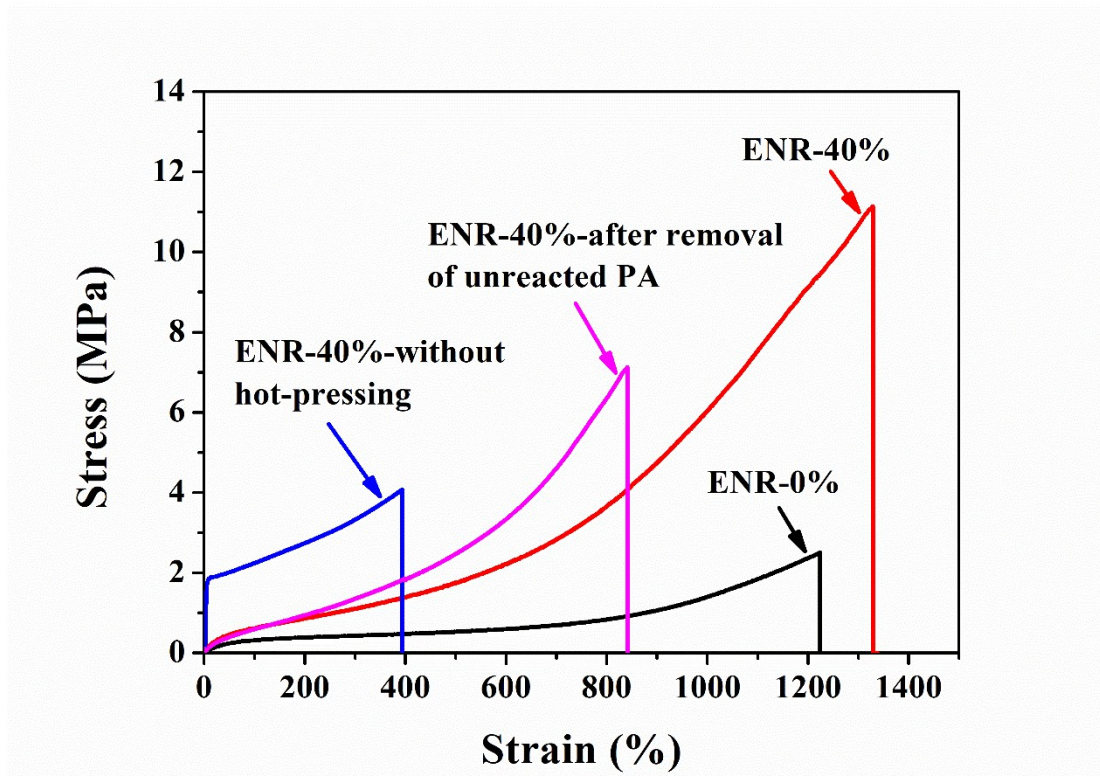
Figure S3. Stress-strain curves for neat ENR, ENR/PA blends without hot-pressing, PA-cured ENR before and after removal of unreacted PA.

Mechanical properties of PA-cured ENR with low expoxidation degree (LENR)
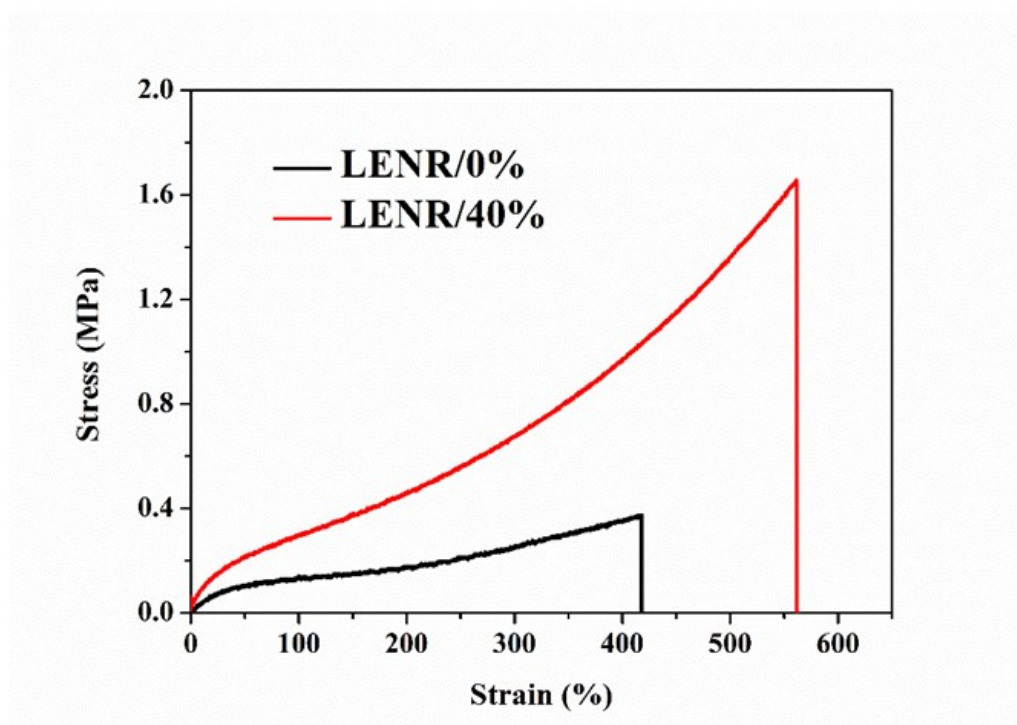
Figure S4. Stress-strain curves for neat LENR and PA-cured LENR.

As shown in **Figure S4**, after cross-linked by PA, the tensile strength and elongation at break of LENR increase to 1.66 MPa and 561.39%, respectively. Obviously, the mechanical properties of PA-cured LENR are much inferior to the ENR with higher epoxidation degree due to the insufficiency of epoxy groups and less multifunctional PA grafted on the ENR chains.

TGA
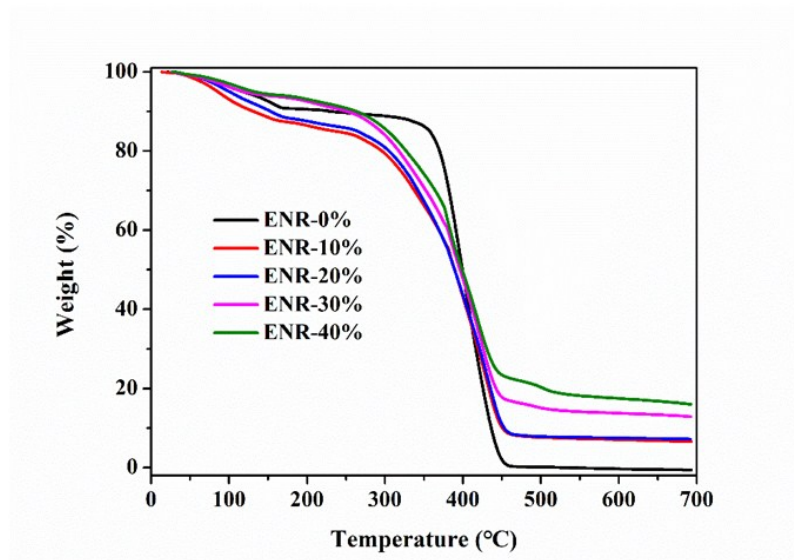
Figure S5. Thermal gravimetric curves of PA-cured ENR.

In the view of the importance of thermal stability for the practical application of flame retardant materials, the thermal decomposition of the PA-cured ENR was investigated by TGA analysis and compared with neat ENR. As shown in **Figure S5**, a slight weight loss occurs at relative low temperature (<100 °C) for both of samples due to the loss of moisture. The stage of weight loss around 200-300 °C can be attributed to the degradation of PA with generation of phosphoric acid. The starting decomposition temperature of the PA-cured ENR is lower than that of neat ENR. This may be attributed to the phosphoric acid speed up the formation of carbonization layer. Noticeably, the residual carbon yield increases remarkably with increasing the content of PA. As a result, the presence of PA facilitates the formation of carbon and prevents materials from catching fire.
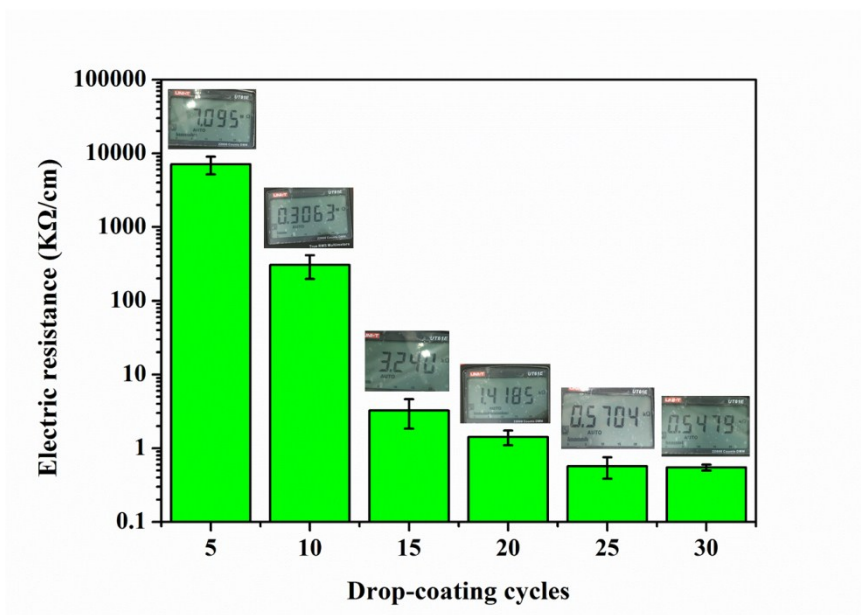
Figure S6. Variation of electric resistance with different drop-coating cycles and the inset pictures are the corresponding gauge reading.

The relationship between the electric resistance and the deposition layers was investigated and showed in **Figure S6**. Gradual drop in electric resistance can be observed with increasing coating numbers. When 25 drop-casting cycles are achieved, the electric sensor attains an electric resistance of 0.57 kΩ per centimeter and the variation in resistance becomes placid with further increase of coating cycles, indicating the formation of nanostructured conductive networks.

Laser scanning confocal microscopy (LSCM)
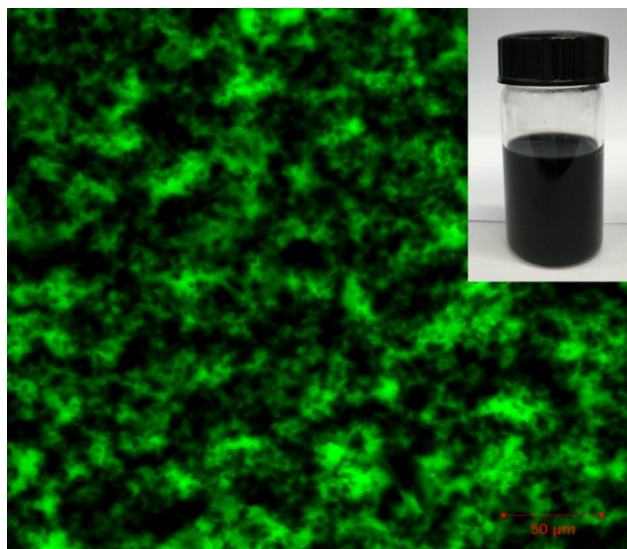
Figure S7. LSCM images of rhodamine-labeled CNC/NR suspension, inset picture gives the digital picture of CNTs@CNC/ENR suspension.

To reveal the structure variation of the nanostructured conductive layer, NR was employed to act as the analogue of ENR which would influence the fluorescent labeling of CNC. Firstly, CNC was stained with rhodamine 6G in order to enable their visualization by LSCM. Briefly, 1 mg rhodamine 6G was dissolved in distilled water (1 g) and mixed with 6.17 g CNC suspension (solid content: 50 mg). Owing to the abundant hydroxyl groups and large specific surface area of CNC, the fluorescents were fully adsorbed on the surface of CNC after stirred for 24 h. Then, NR latex was added to the mixture and sonicated for 5 min to form a homogeneous suspension. Several drips of the suspension were dropped to Petri plates and quickly dried in electric oven. After remove the residual water, an ultrathin film with segregated nanostructure network could be obtained for the next measurement. The rhodamine-labeled CNC was excited at 488 nm with a laser attenuation of 5% and the emission light was recorded using band-pass filter to collect wave length between 500-700 nm. The LSCM images were taken at 200× magnification with a pinhole diameter of 1 Å. As shown in **Figure**

S7, a compact segregated nanostructure network is observed, which is consistent with the SEM and TEM micrography.
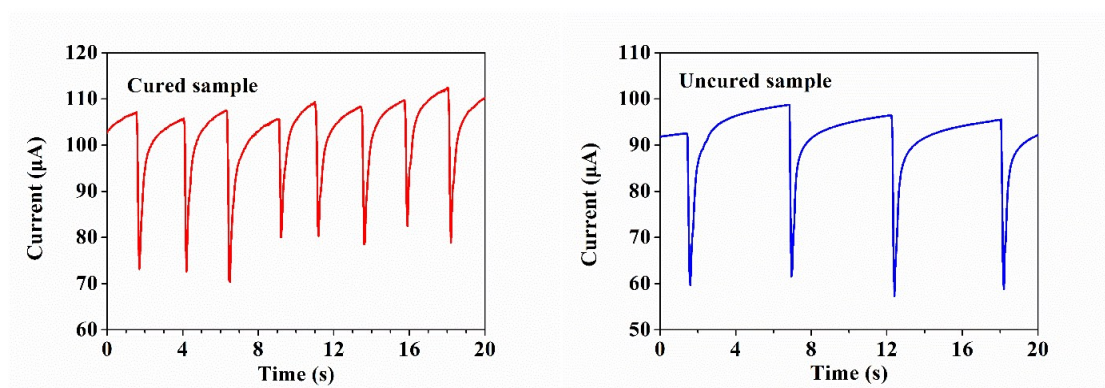
Figure S8. The current variation of finger bending monitored by electronic sensor based on PA-cured ENR (left) and uncured ENR (right).

Large-scale human motion detecting

In order to demonstrate the capabilities of our nanostructured sensor in large strain detecting, it was mounted on the joint of index finger and wrist with medical adhesive tapes. The tester was conducted to perform finger and wrist bending-releasing sequences, as shown in **Figure 5b, 5c**. The current signals show a sharp decrease peak after bending finger and wrist. The larger the motion range is, the higher the peak intensity reach. The results could be attributed to the large-area deformation of conductive network caused by the tensile of sensor. When the index finger or wrist bend, the sensor is stretched and the electric resistance increases abruptly. After releasing the bending, the current gradually recover to its original value. Along with the repeatedly bend, the current patters show no evident changes, suggesting that response behavior of the prepared sensor is repeatable and stable.
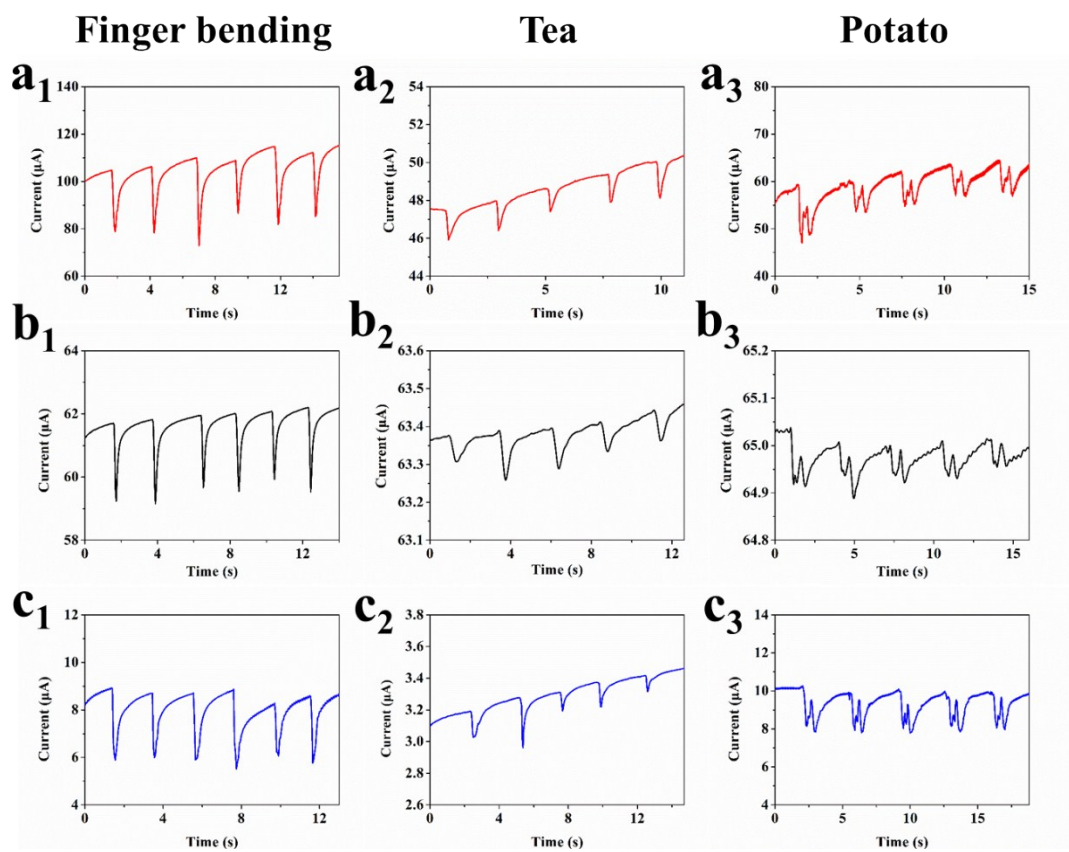
Figure S9. The current variation of finger bending, pronouncing "tea" and "potato" after immersing in normal saline for several minutes (a), accelerated aging test for 7days (b) and placing for 100 days at room temperature (c).

Reference

1. P. J. Flory, *J. Chem. Phys.*, 1950, **18**, 108-111.
2. C. J. Sheehan and A. L. Bisio, *Rubber Chem. Technol.*, 1966, **39**, 149-192.